Journal of the Ceramic Society of Japan 112 [4] 200–203 (2004)

Paper

Effect of Particle Size and Its Distribution on the Fabrication and Magnetic Properties of Barium Ferrite Powders Prepared from Coprecipitated Precursors

Mahmoud Hossny MAKLED, Toshiyuki MATSUI,* Hiroshi TSUDA,* Hiroshi MABUCHI,*
Mabrouk Kamel El-MANSY and Kenji MORII*

Department of Physics, Faculty of Science, Zagazig University, Banha Branch, Banha, Egypt
**Department of Metallurgy and Materials Science, Graduate School of Engineering, Osaka Prefecture University, 1–1, Gakuen-cho, Sakai-shi 599–8531*

共沈法によるバリウムフェライト粉末の作製とその磁気特性に及ぼす粒径分布の影響

M. H. Makled・松井利之*・津田 大*・間渕 博*・M. K. El-Mansy・森井賢二*

Department of Physics, Faculty of Science, Zagazig University, Banha Branch, Banha, Egypt
*大阪府立大学大学院工学研究科材料工学分野，599–8531 堺市学園町 1–1

Six kinds of powder samples with a different particle size and its distribution have been prepared from coprecipitated precursors by light grinding followed by sieving, and calcined in air to form the barium ferrite ($BaFe_{12}O_{19}$) phase. Correlation between the particle morphology and Fe/Ba molar ratio or magnetic properties has been examined. The results indicated that the powders consisting of coarse particles (100–200 μm) exhibit a single phase of $BaFe_{12}O_{19}$, and a higher saturation magnetization and coercivity than the powders having fine particles or a wide size distribution. The optimized powders showed a high coercivity of 5.85 kOe and a saturation magnetization of 71 emu/g that are closed to the theoretical values.

[Received October 30, 2003; Accepted January 23, 2004]

Key-words : *Barium ferrite, Particle size, High coercivity, Porosity, Coprecipitation*

1. Introduction

Hexagonal barium ferrite ($BaFe_{12}O_{19}$) is amongst the most widely used material for permanent hard magnet applications since its discovery. This is owing to its large coercivity and saturation magnetization, high Curie temperature, excellent chemical stability together with high magnetic stability, corrosion resistivity and low prices.[1),2)] To overcome milling processes and to avoid undesirable chemical inhomegeniety of particles in a conventional ceramic processing, chemical coprecipitation is one of suitable methods for producing the barium ferrite powders of appropriate properties in a lower cost. The most important feature of this method is the intimate mixing of the starting materials on an ionic level, so that subsequent nucleation and crystallization can occur at a relatively low temperature.[3)] The following preparation parameters are usually taken into account to fabricate the barium ferrite powders by coprecipitation methods; (1) starting Fe/Ba molar ratio n,[4),5)] (2) pH of solution,[3),5)] (3) sequence of reagent addition,[6)] (4) presence of NaCl,[7)] (5) grinding level of precursors (particle size),[3),8),9)] (6) calcination temperature,[4),10),11)] (7)-time,[12)] (8)-atmosphere (oxygen or air), and (9) addition of protective agents.[10),13)] Here, we can point out two additional important parameters that affect the crystallization process of the precursor; (10) a particle size and its distribution and (11) a final Fe/Ba molar ratio in the precursor, which are not taking into account widely, except for the case of ultra fine powders.[9)] Therefore, it is important to study all these preparation parameters in detail for synthesizing the barium ferrite powders with high quality.

The aim of this work is to prepare chemically homogeneous aggregates of the barium ferrite powders having a high coercivity together with a good saturation magnetization by selecting and controlling the preparation parameters mentioned above. All these parameters were experimentally optimized so as to increase the magnetic properties. In this report, special attention was paid on the parameters (5), (10) and (11).

2. Experimental procedure

Both iron chloride [$FeCl_3 \cdot 6H_2O$] and barium chloride [$BaCl_2 \cdot 2H_2O$] were used as starting materials. The eleven preparation-parameters mentioned above and the experimental sequence optimized in this work are explained as follows: (1) The starting Fe/Ba molar ratio n is equal to 11, (2) pH = 12, (3) [$NaOH$–Na_2CO_3] solution was added to the [$FeCl_3$–$BaCl_2$] solution, and (4) the resultant precursor was washed carefully by hot distilled water to eliminate all the residual sodium chloride. (5) The precursor was subjected to light hand-grinding, and (6) the obtained powders were calcined at a temperature ranging from 900 to 1000°C, (7) for 1.5 h, (8) in flowing air, (9) without adding protective agents. After hand grinding the precursor at the experimental sequence (5), (10) the powders were sieved and classified into six groups depending on the size and its distribution (d_{max}/d_{min}) such as shown in **Table 1**. (11) The change in the Fe/Ba molar ratio in the precursor was measured by electron probe microanalysis (EPMA) before calcination.

The barium ferrite powder samples were evaluated by EPMA (JOEL, JAX–879), X-ray diffraction (XRD; Rigaku Roterflex) using Cu Kα and differential thermal analysis (DTA, Shimadzu TAS 100). For the characterization of powder morphology, transmission electron microscopy (TEM) is inadequate for the present samples since the degree of agglomeration of the powders may change during sample preparation by an ultrasonic technique for TEM, so that photomicroscopy was used to investigate the powders. The magnetic properties of the samples were characterized in a

Table 1. Particle Size Classification of the Powder Samples Prepared, Where d_{max} and d_{min} are Maximum and Minimum Particle Size in the Sample, Respectively

Samples	Particle size distribution $d_{max} \sim d_{min}$ (μm)	d_{max}/d_{min}
A	Rough powder (as ground)	>>10
B	> 45	~10
C	200~100	2
D	100~75	1.3
E	75~45	1.7
F	45 >	>10

SQUID (superconducting quantum interference device) magnetometer (Quantum Design MPMS XL) up to a field of 30 kOe.

3. Results and discussion

Since barium hydroxide and ferric hydroxide have a different solubility in water, the precipitation of precursor from these hydroxides will occur in a different rate. This may lead to a change in the Fe/Ba molar ratio n from the starting value,[12] where the optimum reaction temperature may shift as a function of n.[14] So, the molar ratio in the precursor was examined by EPMA. The results indicated that there are no significant changes in the values of n for all the powders with a different size distribution, as shown in **Table 2** for the sample A, C and F. The measured values are nearly the same as the starting ratio $n=11$ and only fluctuating around this value. However the fluctuation increases by reducing the particle size and increasing the size distribution (d_{max}/d_{min}, in Table 1), both of which depend strongly on the preparation and grinding conditions of precursors.

Figure 1 shows the XRD patterns for the sample A (as-ground, wide particle-size distribution) and C (100–200 μm in particle size) before and after calcining at 925 and 920°C, respectively, for 1.5 h. The coprecipitated precursor showed an amorphous nature, and no significant difference was recorded between the two samples A and C. After the heat treatment, the precursor was converted completely into the $BaFe_{12}O_{19}$ phase for the sample C′, whereas undesirable peaks such as Fe_2O_3, $BaFeO_3$, and $BaFe_2O_4$ are observed in the sample A′ having a wide particle-size distribution. In the case of the sample F consisting of fine particles smaller than 45 μm, the XRD pattern coincided completely with that of the sample A. The presence of such additional peaks affects the magnetic properties of the samples, which will be shown later.

Photomicroscopic examination was performed to reveal the difference in powder morphology between the sample A and C. A typical example of microstructure is given in **Fig. 2**. It is clear that there are only small changes in the morphology before and after the calcination. The sample A exhibits a wide particle size distribution and an inhomogeneous particle agglomeration (dense or loose), whereas the sample C shows a homogeneous distribution of coarse particles that provides a porous structure in the precursor. These tendencies seem to be amplified by the calcination as seen in Fig. 2(A), (A′) and (C), (C′), respectively.

As indicated in Table 2, the samples containing fine particles smaller than 45 μm showed a higher fluctuation in the n values than the coarse powder sample. This result can be interpreted by assuming that most of the fine particles are derived by grinding the parts of precursor that are remaining in unachieved formation of chemically homogeneous well developed particles and have an Fe/Ba molar ratio largely fluctuating around the initial value of n. In contrast, the coarse particles greater than about 100 μm are homogeneously coprecipitated with a molar ratio close to the starting value,

Table 2. Variation of Fe/Ba Molar Ratio in the Samples with Different Particle Size Distribution

Samples	Fe/Ba molar ratio n
A	11±3
C	11± 0.2
F	11±2

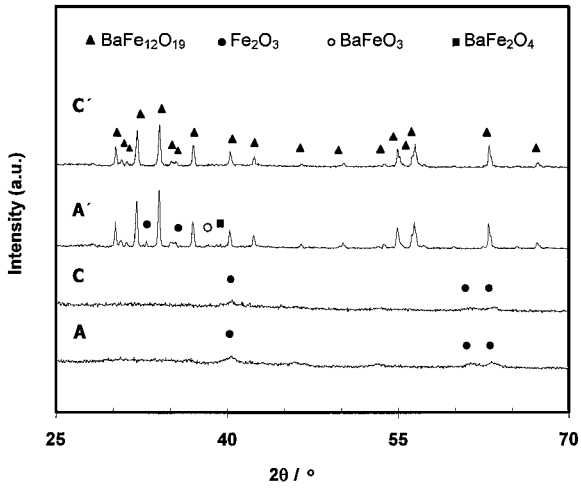

Fig. 1. XRD patterns of the samples (A, A′) and (C, C′) before and after calcination at 925 and 920°C, respectively, for 1.5 h.

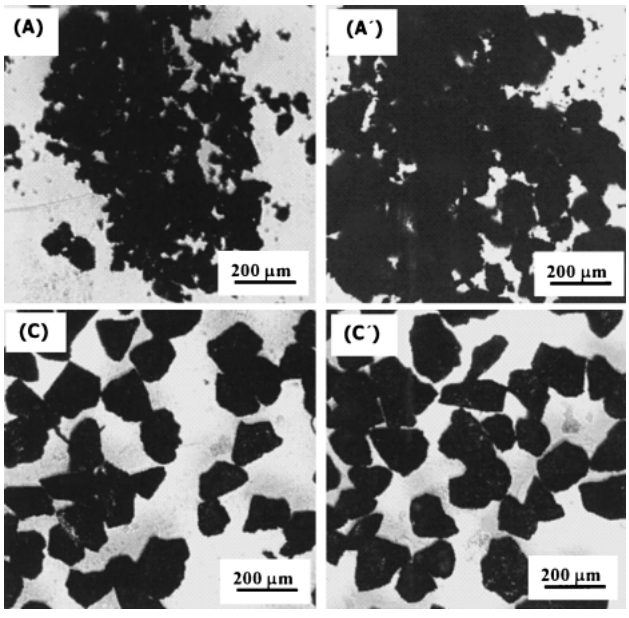

Fig. 2. Photomicrographs of the particles in samples (A, A′) and (C, C′), before and after calcination at 925 and 920°C, respectively, for 1.5 h.

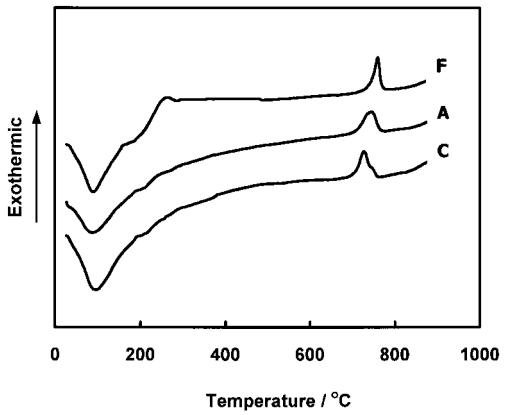

Fig. 3. DTA curves for the samples A, C and F. The exothermic peaks found in a temperature range between 700 and 800°C indicate crystallization of the barium ferrite phase.

suggesting that most coprecipitation reactions were completed in these particles.

DTA curves are shown in **Fig. 3** for the samples A, C and F. The endothermic peaks located below 150°C are attributed to the elimination of absorbed water. The exothermic peak at about 300°C is due to the decomposition of hydroxide and the formation of crystalline oxides.[9] The barium ferrite phase starts to crystallize at about 700°C, and a single-phase material can be obtained after annealing at 900°C or above as reported before.[15] In a temperature range between 700 and 800°C, three distinguished exothermic beaks appeared clearly at 735, 754, and 763°C for the samples C, A, and F, respectively. The difference in the reaction temperatures is attributed to the following differences in the particle morphology of these samples: The sample C consisting of coarse particles may have a homogeneous chemical composition, which is achieved by well coprecipitated larger particles in the precursor resulting in a porous structure supplying sufficient oxygen to crystallize the $BaFe_{12}O_{19}$ phase during calcination. This will lead to the formation of $BaFe_{12}O_{19}$ at a relatively low temperature.[3] On the other hand, rather higher reaction temperatures are recorded in the samples A and F that have fine particles (<45 μm) and a large fluctuation in the Fe/Ba molar ratio ($n=11\pm2$–3). Following two factors could be pointed out for this reason: First, inhomogeneous chemical composition is achieved in the case of fine particles as explained above. Secondly, since the fine particles tend to agglomerate to form dense lumps with a low porosity even after grinding, the amount of oxygen during calcination is deficient inside these agglomerates resulting in the growth of chemically inhomogeneous particles including second phases. Since the powder color is sensitive to the presence of different phases and the concentration of barium ferrite,[16] we observed the color of the samples to confirm the second assumption. The results indicated that the exterior surface of the sample A showed a color of more darkly brown than the interior, whereas in the case of sample C, no significant change in color was recorded between the both surfaces. These results suggest the difficulty in synthesizing the $BaFe_{12}O_{19}$ phase from fine particles obtained by grinding the precursor.

The magnetic properties were measured for all the samples prepared at a temperature ranging from 900 to 1000°C, and the results are listed in **Table 3**. Here, we can clearly notice that the magnetization increases by removing the fine powders

Table 3. Maximum Coercivity (H_c) and Saturation Magnetization (σ) at 30 kOe of the Samples Calcined at the Temperature (T) in a Range 900–1000°C

Samples	T(°C)	H_c(kOe)	σ(emu/g)
A	925	3.84	65
B	925	5.15	67
C	920	5.85	71
D	950	5.63	68
E	970	4.55	59#
F	1000	3.18	65

obtained at 10 kOe

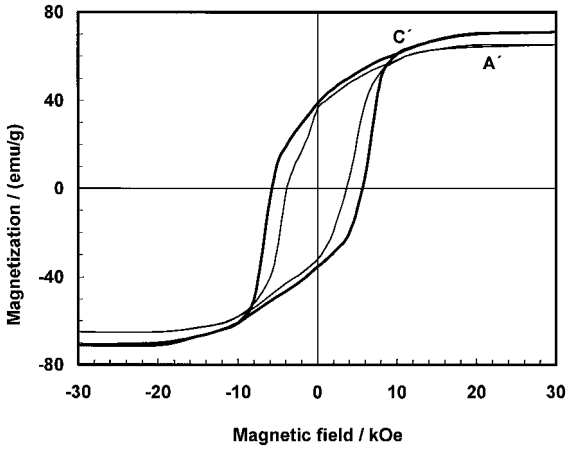

Fig. 4. Hystersis loops of the samples (A′) and (C′) calcined at 925 and 920°C, respectively, for 1.5 h.

smaller than about 45 μm, whereas the coercivity increases with increasing average particle size and reducing the size distribution (d_{max}/d_{min}, in Table 1) i.e. with increasing d_{min}. Accordingly, it is assumed that the porosity characterized by a minimum particle size d_{min} in the aggregates greatly affects the coercivity of the barium ferrite powders. All the samples except C recorded a lower saturation magnetization due to the presence of the second phases as mentioned above.

Figure 4 shows a comparison of the hysteresis curves for the samples A and C. The sample C shows more superior magnetic properties than sample A, and has a saturation magnetization of 71 emu/g and a coercivity of 5.85 kOe. The particle size in sample C is large (100–200 μm) for accommodating the multidomain (about 200 times larger than the domain size).[17] Since a higher coercivity value in barium ferrite powders usually results from the fine particles with a single-domain structure, the following magnetic behavior of the sample C observed in Fig. 4 is worthy to note: (a) The recorded saturation magnetization and coercivity are very close to the theoretical values according to the Stoner–Wohlfarth (SW) curve,[18] and (b) the demagnetization characteristics are similar to those of the single-domain particles reported in literatures.[6),19] These may be rationalized by speculating that the coarse particles in this sample are consisting of fine crystallites operating as a single-domain structure. According to the discussion given in foregoing sections, the magnetic properties of the sample C are basically determined by the geometrical factor of particle distribution in the precursor

during crystallization, and therefore the microstructures developed in the final particles. More detailed microstructural examinations are required to confirm this view.

4. Conclusions

The present results clearly demonstrate that the process consisting of both light grinding and sieving of coprecipitated presursors is useful for obtaining chemically homogeneous coarse particles with a narrow size distribution, which exhibit superior magnetic properties. The samples having fine particles are a mixture of the hard phase [$BaFe_{12}O_{19}$], soft phase [$BaFe_2O_4$] and eventually no magnetic phases. This is due to a large fluctuation in the Fe/Ba molar ratio and the agglomeration of fine particles, which lead to an oxygen deficient crystallization resulting in second phases formation. In contrast, the sample consisting of large particles (100–200 μm) precipitates with a homogeneous chemical composition ($n = 11 \pm 0.2$), forms a porous precursor, and transforms into the single phase of $BaFe_{12}O_{19}$ after calcination. It is concluded from the magnetic measurements that the porosity rather than the average particle size affects the magnetic properties of the barium ferrite powders. The recorded-coercivity and -saturation magnetization are very closed to the theoretical values.

Acknowledgements The authors would like to express their deep gratitude to Mr. Atsushi Kakitsuji, Mr. Yoshiaki Sakamoto and Mr. Kazuhiko Yamamoto, Technology Research Institute of Osaka Prefecture, for their valuable help.

References

1) Kojima, H., "Ferromagnetic Materials," Vol. 3, Ed. by Wohlfarth, E. P., North-Holland (1982) pp. 305–307.
2) Liu, X., Wang, J., Gan, L. M. and Ng, S. C., *J. Magn. Magn. Mater.*, Vol. 195, pp. 452–459 (1999).
3) Haneda, K., Miyakawa, C. and Kojima, H., *J. Am. Ceram. Soc.*, Vol. 57, pp. 354–357 (1974).
4) Roos, W., *J. Am. Ceram. Soc.*, Vol. 63, pp. 601–603 (1980).
5) Janasi, S. R., Rodrigues, D., Landgraf, F. J. G. and Emura, M., *IEEE Trans. Magn.*, Vol. 36, pp. 3327–3329 (2000).
6) Janasi, S. R., Emura, M., Landgraf, F. J. G. and Rodrigues, D., *J. Magn. Magn. Mater.*, Vol. 238, pp. 168–172 (2002).
7) Janasi, S. R., Rodrigues, D., Emura, M. and Landgraf, F. J. G., *Phys. Stat. Sol.* (a), Vol. 185, pp. 479–485 (2001).
8) Hong, Y. K., Paig, Y. J., Agresti, D. G. and Shelfer, T. D., *J. Appl. Phys.*, Vol. 61, pp. 3872–3874 (1987).
9) Liu, X., Wang, J., Ding, J., Chen, M. S. and Shen, Z. X., *J. Mater. Chem.*, Vol. 10, pp. 1745–1749 (2000).
10) Ng, W. K., Ding, J., Chow, Y. Y., Wang, S. and Shi, Y., *J. Mater. Res.*, Vol. 15, pp. 2151–2156 (2000).
11) Wang, S., Ding, J., Shi, Y. and Chen, Y. J., *J. Magn. Magn. Mater.*, Vol. 219, pp. 206–212 (2000).
12) Castro, S., Gyosa, M., Rodriguez, C., Rivas, J., Mira, J. and Greneche, J. M., *J. Magn. Magn. Mater.*, Vol. 152, pp. 61–69 (1996).
13) Chen, D. H. and Chen, Y. Y., *J. Colloid Inter. Sci.*, Vol. 235, pp. 9–12 (2001).
14) Melzer, K. and Martin, A., *Phys. Stat. Sol.* (a), Vol. 107, pp. K163–K166 (1988).
15) Ding, J., Tsuzuki, T. and McCormick, P. G., *J. Magn. Magn. Mater.*, Vol. 177, pp. 931–932 (1998).
16) Affleck, L., Aguas, M. D., Parkin, I. P., Pankhurst, Q. A. and Kuznetsov, M. V., *J. Mater. Chem.*, Vol. 10, pp. 1925–1932 (2000).
17) Tenzer, P. K., *J. Appl. Phys.*, Vol. 34, pp. 1267–1270 (1963).
18) Stoner, E. C. and Wohlfarth, E. P., *Phil. Trans. Roy. Soc.*, Vol. A240, pp. 599–642 (1948).
19) Haneda, K. and Kojima, H., *J. Appl. Phys.*, Vol. 44, pp. 3760–3762 (1973).